MASTER THESIS

A New Definition of the Tunneling Time

トンネリング時間の新しい定義

Yusuke Aoki

青木佑介

(35102001)

Department of Physics,
Graduate School of Science and Engineering,
Aoyama Gakuin University

Supervisors: Kenn Kubo and Naomichi Hatano
指導教官：久保健・羽田野直道

2003

論　文　要　旨
(和　文)

提 出 年 度： 2003
提　出　日： 2004/02/10
専　　攻： 物理学
学 生 番 号： 35102001
学 生 氏 名： 青木佑介
研究指導教員：久保健・羽田野直道

(論文題目)
トンネリング時間の新しい定義

(内容の要旨)
新たなトンネリング時間の定義を提唱する。トンネリング時間とは、粒子がトンネル障壁を通過するのにかかる時間である。トンネリング時間の定義には様々なものがあり、波束を用いて定義したものやファインマンの径路積分を用いたもの、トンネル障壁を振動させて時間を定義するものなどがある。しかしどれが正しいか定かではなく、そもそも、そのような時間を定義できるのかもわかっていない。現在盛んな議論が行われているところである。我々は新たな定義として共鳴状態の寿命を用いる。幾つかのポテンシャルについて実際に計算した結果も報告する。

実験との比較を考慮し、三角のポテンシャルにおける共鳴状態を求めた。すると、ポテンシャルよりもエネルギーの小さい範囲において共鳴状態が幾つか見つかった。我々は、これら共鳴状態のエネルギー固有値の虚部の逆数がトンネリング時間に相当すると考える。更にエネルギーに対する透過係数を求めた。その結果、ある一つの共鳴状態が影響していると思われるピークが見つかった。

共鳴状態の寿命（共鳴状態の固有値の虚部の逆数）はポテンシャルに閉じ込められた電子が共鳴散乱によってポテンシャルの外に出ていくまでの時間である。トンネル障壁のある系にも共鳴状態があれば、その寿命がトンネリング時間を表すと考える。

我々はその共鳴状態を求めるために、「系の遠方において外向波のみ存在する」という境界条件を用いて、シュレーディンガー方程式を解析的に解いた。共鳴状態は通常、散乱を表す行列である S 行列を用いて求めることができる。共鳴状態を求める手法として、上で述べた境界条件を用いて解く手法と S 行列を用いる手法が実は等価であることを説明する。またそこから求められる共鳴状態の固有値は一般的に複素数である。なぜなら、上述した境界条件で系から出ていく運動量の流束がハミルトニアンの期待値の虚部と比例するからである。

Academic Year of 2003, Submitted on Feb.25, 2004

Graduate School of Science and Engineering, Aoyama Gakuin University

A New Definition of the Tunneling Time

Yusuke Aoki (35102001)
Department of Physics
Supervisors: Kenn Kubo and Naomichi Hatano

We propose a new definition of the tunneling time. The tunneling time is the time that it takes for a particle to pass through a tunneling barrier. Various definitions of the tunneling time have been proposed [1], including the ones that use a wave packet [2], the Feynman path integral [3] and an oscillatory barrier [4]. However, it is controversial which definition is the most appropriate. We here define the tunneling time using the lifetime of resonant states. We present results obtained for several types of potential.

We first search resonant states in a triangular potential, which may be comparable to experimental situations. We find resonant states, some of which are located inside the potential. We propose to define the tunneling time as the reciprocal of the imaginary part of the resonant eigenvalue. We note that the resonant states inside the potential do not move when the potential width and height are changed, while keeping the potential slope unchanged. We also show resonant states in other potentials. For a potential with a flat top, we find resonant states inside the potential, similar to the case of the triangular potential. The resonant states inside the potential do not move at all when the potential width is changed. We also find resonant states inside a semi-infinite potential, whereas there are not any states located above the potential.

We calculated the energy dependence of the transmission probability as well. A peak appears in the transmission probability owing to a resonant state. We discuss the relation between the position of resonant states and the peak in the transmission probability.

[1] R. Landauer and T. Martin, *Barrier interaction time in tunneling*, Rev. Mod. Phys. **66**, 217-228 (1994)
[2] e.g. T. E. Hartman, J. Appl. Phys. **33**, 3427 (1962)
[3] D. Sokolovski and L. M. Baskin, *Traversal time in quantum scattering*, Phys. Rev. A **36**, 4604 (1987)
[4] M. Büttiker and R. Landauer, *Traversal time for tunneling*, Phys. Rev. Lett. **49**, 1739 (1982)

MASTER THESIS
A New Definition of the Tunneling Time

Yusuke Aoki
(35102001)
Department of Physics,
Graduate School of Science and Engineering,
Aoyama Gakuin University
5-10-1 Fuchinobe, Sagamihara, Kanagawa 229-0006, Japan

Supervisors: Kenn Kubo and Naomichi Hatano

February 25, 2004

Abstract

We propose a new definition of the tunneling time using the lifetime of resonance states. For several types of potentials, we find resonance states, some of which are located inside the potential. We show the tunneling time calculated from the lifetime of these states. We also show the energy dependence of the transmission probability.

Contents

1 Introduction

The tunneling time is the time that it takes for a particle to pass through a tunneling barrier. Various definitions of the tunneling time have been proposed [1]. However, it is controversial which definition is the most appropriate. One of the definitions, for example, is based on the use of a wave packet [2]. It measures the time that takes for a transmission wave packet to come out of the barrier since an incident wave packet comes into it. This definition of the tunneling time, however, have met the following counterargument [1]. The transmission probability of a wave is generally greater for a greater wave number. The above definition of the tunneling time hence measures only the tunneling time of a wave component with the greatest wave number. Another definition of the tunneling time uses the Feynman path integral [3], and the Büttiker-Landauer time [4] uses an oscillatory barrier.

In the present thesis, we propose to define the tunneling time using the lifetime of resonant states. We present our definition of the tunneling time in Section 2. Since we use the lifetime of resonant states for the definition, we review in Section 3 a few properties of resonant states. In particular, we discuss the relation between complex eigenvalues and the momentum flux in Section 3.1. We show that an eigenvalue is generally complex, if the momentum in a system is not preserved. In Section 3.2, we discuss the lifetime of the resonant state by using the time-dependent Schrödinger equation. We propose to define the tunneling time as the reciprocal of the imaginary part of the resonant eigenvalue. In Section 3.3, we introduce a special boundary condition for searching resonant states: only the outgoing wave exists in the limit $|x| \to \infty$. We show that using this boundary condition is equivalent to searching singularities of the scattering matrix.

We present our numerical results in Section 4. We first search resonant states in a triangular potential. This potential may be comparable to experimental situations. We find resonant states, some of which are located inside the potential. We also show resonant states in other potentials as well as the energy-dependence of the transmission probability. A peak appears in the transmission probability owing to a resonant state. We discuss the relation between the position of resonant states and the peak in the transmission probability.

2 The tunneling time defined by using the lifetime of resonant states

In the present section, we propose a new definition of the tunneling time by using the lifetime of resonant states. Hereafter, we focus on problems in one dimension.

Consider a resonant state shown in Fig. 1. An electron is trapped in a

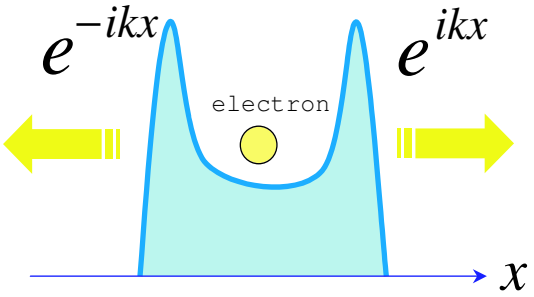

Figure 1: A resonant state.

potential for a while and eventually escapes from the potential. This is the resonant scattering. The lifetime of the resonant state is the time that it takes for the trapped electron to go out of the potential.

Now as a gedanken experiment, suppose that we raise the bottom of the potential as shown in Fig. 2. We can regard the rectangular potential as a limit of the trapping potential. Resonant states that are trapped in the potential may survive in the rectangular potential. The lifetime τ of the possibly surviving resonant state is the time it takes for a particle virtually "trapped" inside the rectangular potential to go out of the potential. Thus we propose to define the tunneling time as twice the resonant lifetime; τ to get into the potential and further τ to get out of it.

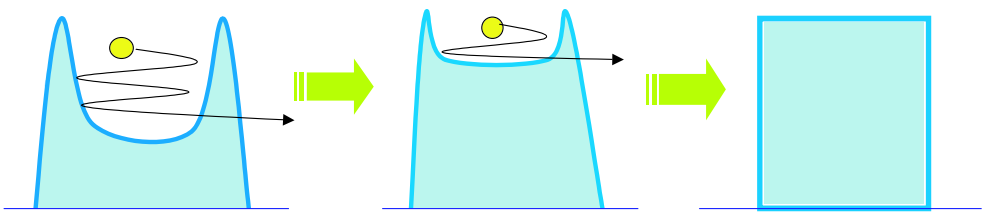

Figure 2: A rectangular potential as a limit of a trapping potential.

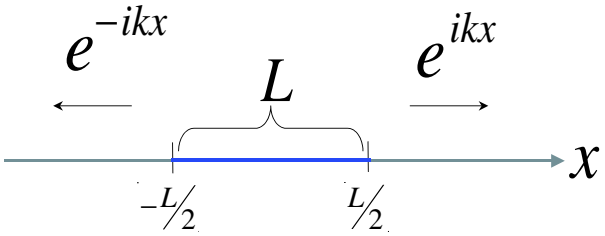

Figure 3: A segment of the length L.

3 The theoretical explanation

Since we use the resonant state for the definition of the tunneling time, we here review a few theoretical aspects of the complex eigenvalue of the resonant state.

3.1 Complex eigenvalues and the momentum flux

In the present subsection, we discuss the relation between complex eigenvalues and the momentum flux [5]. We show that the eigenvalues of a system where the momentum is not preserved can be generally complex.

Let us consider a Hamiltonian in one dimension,

$$\mathcal{H} = K + V, \tag{1}$$

where the kinetic energy K is given by

$$K \equiv \frac{p^2}{2m} = -\frac{\hbar^2}{2m}\frac{\partial^2}{\partial x^2}, \tag{2}$$

and the (real) potential

$$V = V^* \tag{3}$$

is reasonably concentrated around the origin. Let us define the expectation value of the Hamiltonian as

$$\langle\psi|\mathcal{H}|\psi\rangle_L \equiv \int_{-L/2}^{L/2} \psi(x)^* \mathcal{H}\psi(x)dx. \tag{4}$$

Note that we define the expectation value on a segment of length L as shown in Fig. 3. We obtain the usual definition of the expectation value in the limit $L \to \infty$. The reason of the unusual definition (4) will be self-evident

below. We show now that the imaginary part of the expectation value of the Hamiltonian exists. The complex conjugate of Eq. (4) is

$$(\langle\psi|\mathcal{H}|\psi\rangle_L)^* \equiv \int_{-L/2}^{L/2} \psi(x)\mathcal{H}^*\psi(x)^* dx. \tag{5}$$

Subtracting Eq. (5) from Eq. (4), we have

$$2i\mathrm{Im}\langle\psi|\mathcal{H}|\psi\rangle_L = \langle\psi|\mathcal{H}|\psi\rangle_L - (\langle\psi|\mathcal{H}|\psi\rangle_L)^* = \langle\psi|K|\psi\rangle_L - (\langle\psi|K|\psi\rangle_L)^*. \tag{6}$$

Note that the potential term vanishes because it is Hermitian. The right-hand side of Eq. (6) is transformed by partial integration as follows:

$$\begin{aligned}
&\langle\psi|K|\psi\rangle_L - (\langle\psi|K|\psi\rangle_L)^* && (7)\\
= \quad & -\frac{\hbar^2}{2m}\left[\psi(x)^*\frac{\partial}{\partial x}\psi(x)\right]_{-L/2}^{L/2} + \frac{\hbar^2}{2m}\int_{-L/2}^{L/2}\frac{\partial}{\partial x}\psi(x)^*\frac{\partial}{\partial x}\psi(x)dx \\
& +\frac{\hbar^2}{2m}\left[\psi(x)\frac{\partial}{\partial x}\psi(x)^*\right]_{-L/2}^{L/2} - \frac{\hbar^2}{2m}\int_{-L/2}^{L/2}\frac{\partial}{\partial x}\psi(x)\frac{\partial}{\partial x}\psi(x)^*dx \\
= \quad & -\frac{i\hbar}{2m}\left[\psi(x)^*p\psi(x) + \psi(x)(p\psi(x))^*\right]_{-L/2}^{L/2} \\
= \quad & -\frac{i\hbar}{m}\mathrm{Re}\left(\left[\psi(x)^*p\psi(x)\right]_{-L/2}^{L/2}\right), && (8)
\end{aligned}$$

where we used

$$p \equiv \frac{\hbar}{i}\frac{\partial}{\partial x}. \tag{9}$$

Thus we have

$$2\mathrm{Im}\langle\psi|\mathcal{H}|\psi\rangle_L = -\frac{\hbar}{m}\mathrm{Re}\left(\langle\psi|p|\psi\rangle_{x=L/2} - \langle\psi|p|\psi\rangle_{x=-L/2}\right), \tag{10}$$

where

$$\langle\psi|p|\psi\rangle_{x=L/2} \equiv \psi(L/2)^* p\psi(L/2), \tag{11}$$

is the momentum flux at $x = L/2$, and $\langle\psi|p|\psi\rangle_{x=-L/2}$ is defined likewise. The right-hand side of Eq. (10) means the total momentum flux which goes out of the segment of length L. Thus eigenvalues can be generally complex when the momentum is not conserved as in the situation in Fig. 1. In fact, we define resonant states using the boundary condition where only the outgoing waves exist in the limit $|x| \to \infty$, as we see below.

3.2 The lifetime of resonant states

In the present subsection, we discuss the relation between the lifetime τ of resonant states and the imaginary part Γ of the corresponding complex eigenvalues

$$E = E_r - i\frac{\Gamma}{2}, \tag{12}$$

namely the relation

$$\tau \equiv \frac{\hbar}{\Gamma}. \tag{13}$$

We first consider the time-dependent Schrödinger equation

$$i\hbar\frac{\partial}{\partial t}\Psi(x,t) = \left\{\frac{p^2}{2m} + V(x)\right\}\Psi(x,t). \tag{14}$$

We assume a solution of the form of the variable separation:

$$\Psi(x,t) = \psi(x)\chi(t). \tag{15}$$

This gives us a set of equations

$$i\hbar\frac{d}{dt}\chi(t) = E\chi(t), \tag{16}$$

$$\left\{\frac{p^2}{2m} + V(x)\right\}\psi(x) = E\psi(x). \tag{17}$$

The solution of Eq. (16) is given by

$$\chi(t) = Ce^{-\frac{i}{\hbar}Et}, \tag{18}$$

where C is a constant. By substituting Eq. (18) for $\chi(t)$ in Eq. (15), we have

$$\Psi(x,t) = Ce^{-\frac{i}{\hbar}Et}\psi(x). \tag{19}$$

Now, suppose that the stationary Schrödinger equation (17) has a complex eigenvalue

$$E = E_r - i\frac{\Gamma}{2}. \tag{20}$$

Then we have

$$\Psi(x,t) = Ce^{-\frac{i}{\hbar}(E_r - i\frac{\Gamma}{2})t}\psi(x). \tag{21}$$

Integrating the square modulus of Eq. (21) over the segment in Fig. 3, we arrive at

$$\int_{-L/2}^{L/2} |\Psi(x,t)|^2 dx = |C|^2 e^{-\frac{\Gamma}{\hbar}t}\langle\psi|\psi\rangle_L. \tag{22}$$

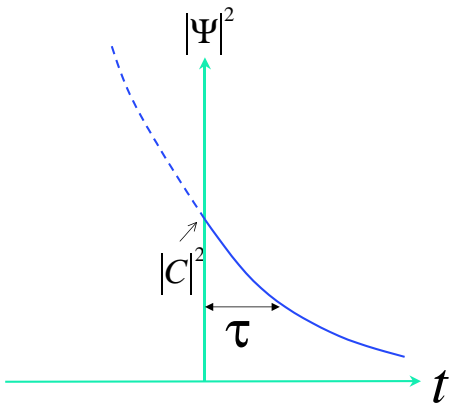

Figure 4: The lifetime of a resonant state.

We can see that the existence probability of a particle in the segment decays exponentially (Fig. 4). The lifetime of the decay is given by $\tau = \hbar/\Gamma$. This is the time it takes for the particle to go out of the trapped potential.

According to the argument in the previous section, the decay rate Γ is related to the momentum flux as

$$\Gamma = -2 \lim_{L\to\infty} \mathrm{Im}\langle\psi|\mathcal{H}|\psi\rangle_L = \frac{\hbar}{m} \lim_{L\to\infty} \mathrm{Re}\left(\langle\psi|p|\psi\rangle_{x=L/2} - \langle\psi|p|\psi\rangle_{x=-L/2}\right). \tag{23}$$

This is indeed a very natural consequence; the decay rate of the existence probability in the segment is proportional to the momentum flux going out of the segment.

3.3 The boundary condition for resonant states

In the present subsection, we discuss the boundary condition for searching resonant states [5].

The resonant state is generally defined as a point in the complex energy plane where the elements of the scattering matrix (or in short, the S matrix) is divergent:

$$S \equiv \begin{bmatrix} R(E) & T(E) \\ T(E) & R(E) \end{bmatrix} \to \infty, \tag{24}$$

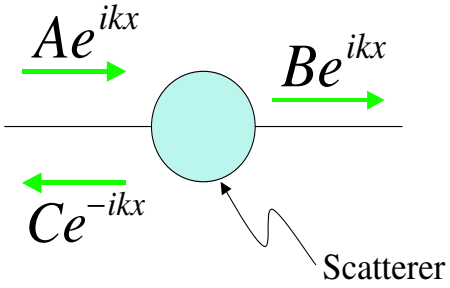

Figure 5: A scattering problem, where Ae^{ikx} is the incident wave, Be^{ikx} is the transmission wave, and Ce^{-ikx} is the reflection wave.

where $R(E)$ and $T(E)$ are the reflection and transmission coefficients, respectively. Instead of the S matrix, however, we use the boundary condition where only the outgoing waves exist in the limit $|x| \to \infty$, in order to search resonant states. We show here that the latter is equivalent to the former. Thus we can search resonant states more easily.

Let us consider a scattering problem as shown in Fig. 5. We assume that an incident wave e^{ikx} with the coefficient $A(E)$ comes in to a scatterer, where

$$k \equiv \frac{\sqrt{2mE}}{\hbar}. \tag{25}$$

After the incident wave is scattered, it is separated into a transmission wave e^{ikx} with the coefficient $B(E)$ and a reflection wave e^{-ikx} with the coefficient $C(E)$. In this case, the S matrix is given by

$$S = \begin{bmatrix} \dfrac{C(E)}{A(E)} & \dfrac{B(E)}{A(E)} \\ \dfrac{B(E)}{A(E)} & \dfrac{C(E)}{A(E)} \end{bmatrix}. \tag{26}$$

The location of the resonant state, or the divergence of the matrix elements is hence given by [6]

$$A(E) = 0. \tag{27}$$

The condition $A(E) = 0$ means that only the outgoing waves exist in Fig. 5. Thus we can use the boundary condition Eq. (27) instead of seeking the divergence of the S matrix in order to search resonant states.

It is now obvious from the arguments in the preceding sections that the resonant states have complex eigenvalues. Since the incoming wave is lacking

as in Eq. (27), the momentum flux is going out of the scatterer. Equation (23) gives the imaginary part of the resonant eigenvalues as

$$\Gamma = -2\mathrm{Im}E = \frac{\hbar^2 k}{m}(|B|^2 + |C|^2) > 0. \tag{28}$$

(Note that the coefficients B and C have the dimensionality of $\sqrt{k}$.)

4 The results

We here present resonant states obtained for several types of potential.

4.1 A triangular potential

We first show resonant states and their lifetimes in a triangular potential shown in Fig. 6, which may be comparable to an experimental situation of the field emission as in Fig. 7. By applying a strong electric field to the tip of a material such as metals and semiconductors, the triangular potential emerges, as shown in Fig. 7(b). An electron near the Fermi surface is eventually emitted out of the potential because of the tunneling effect. We may be able to measure experimentally the time Δt it takes for the electron to pass through the potential.

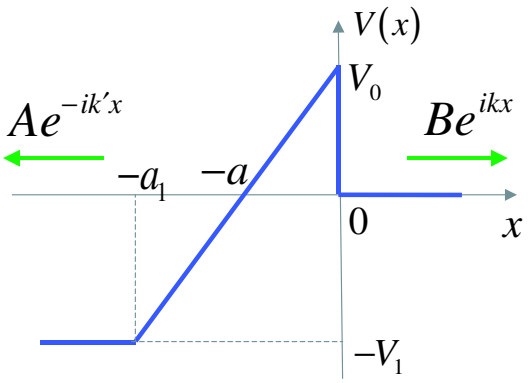

Figure 6: A triangular potential. The potential parameters a, a_1, V_0 and V_1 are all positive.

Let us solve the Schrödinger equation

$$\left\{-\frac{\hbar^2}{2m}\frac{\partial^2}{\partial x^2}+V(x)\right\}\psi(x)=E\psi(x), \tag{29}$$

where the potential is given by

$$V(x)=\begin{cases} -V_1 & (x<-a_1) \\ \frac{V_0}{a}x+V_0 & (-a_1\le x\le 0) \\ 0 & (x>0) \end{cases}, \tag{30}$$

with

$$a_1\equiv\frac{V_0+V_1}{V_0}a. \tag{31}$$

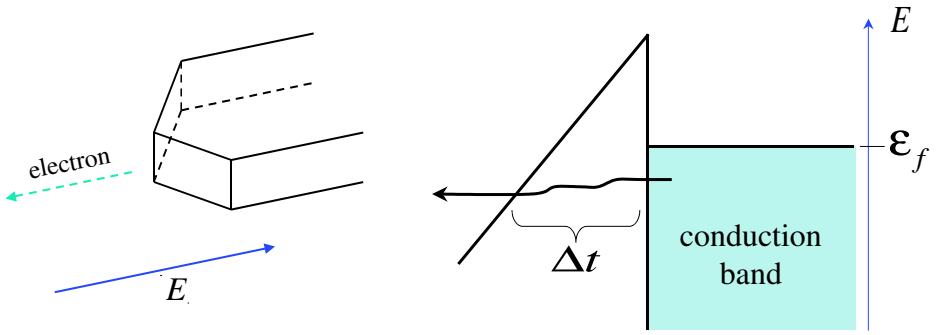

(a) (b)

Figure 7: An experiment situation of the field emission.

(i) In the region $x < -a_1$, Eq. (29) is reduced to

$$\left\{-\frac{\hbar^2}{2m}\frac{\partial^2}{\partial x^2} - V_1\right\}\psi_1(x) = E\psi_1(x). \tag{32}$$

The solution is given by

$$\psi_1(x) = \beta e^{-ik'x}, \tag{33}$$

where β is a constant and

$$k' \equiv \frac{\sqrt{2m(E+V_1)}}{\hbar}. \tag{34}$$

Note that we here used the boundary condition of the outgoing waves only in order to search resonant states. Hence in this region, we have only, the left-going wave in Eq. (33).

(ii) In the region $-a_1 \leq x \leq 0$, we transform the Schrödinger equation in the form

$$\frac{\partial^2\psi_2(x)}{\partial x^2} = f(x)\psi_2(x), \tag{35}$$

where

$$\begin{aligned} f(x) &= -\frac{2m}{\hbar^2}\left(E - V(x)\right) \\ &= -\frac{2m}{\hbar^2}\left(E - \frac{V_0}{a}x - V_0\right) \end{aligned} \tag{36}$$

with

$$f(x) = \alpha(x+X), \tag{37}$$

$$\alpha \equiv \frac{2mV_0}{\hbar^2 a}, \tag{38}$$

$$X \equiv a - \frac{a}{V_0}E. \tag{39}$$

Putting

$$z \equiv \alpha^{\frac{1}{3}}(x+X), \tag{40}$$

we arrive at

$$\frac{\partial^2 \psi_2(x)}{\partial z^2} = z\psi_2(x). \tag{41}$$

Two particular solutions of Eq. (41) are given by the Airy functions

$$A_i(z) = \frac{1}{\pi}\int_0^\infty \cos(\frac{t^3}{3}+zt)dt, \tag{42}$$

$$B_i(z) = \frac{1}{\pi}\int_0^\infty \left\{ e^{-\frac{t^3}{3}+zt} + \sin(\frac{t^3}{3}+zt) \right\}. \tag{43}$$

The general solution $\psi_2(x)$ in this region is a superposition of the two Airy functions:

$$\psi_2(x) = \gamma A_i + \delta B_i, \tag{44}$$

where γ and δ are constants.

(iii) In the region $x > 0$, Eq. (29) is

$$-\frac{\hbar^2}{2m}\frac{\partial^2 \psi_3(x)}{\partial x^2} = E\psi_3(x). \tag{45}$$

The solution is

$$\psi_3(x) = \epsilon e^{-ikx}, \tag{46}$$

where ϵ is a constant and

$$k \equiv \frac{\sqrt{2mE}}{\hbar}. \tag{47}$$

We have only the right-going wave because of the boundary condition for resonant states.

Now we fix the constants β, γ, δ and ϵ with the boundary conditions at $x = -a_1$ and $x = 0$. The boundary conditions at $x = -a_1$ are

$$\psi_1(-a_1) = \psi_2(-a_1), \tag{48}$$
$$\psi_1^{'}(-a_1) = \psi_2^{'}(-a_1), \tag{49}$$

or

$$\beta e^{ik^{'}a_1} = \gamma A_i|_{x=-a_1} + \delta B_i|_{x=-a_1}, \tag{50}$$
$$-ik^{'}\beta e^{ik^{'}a_1} = \gamma A_i^{'}|_{x=-a_1} + \delta B_i^{'}|_{x=-a_1}. \tag{51}$$

Similarly, the boundary conditions at $x = 0$ are

$$\psi_2(0) = \psi_3(0), \tag{52}$$
$$\psi_2^{'}(0) = \psi_3^{'}(0), \tag{53}$$

or

$$\gamma A_i|_{x=0} + \delta B_i|_{x=0} = \epsilon, \tag{54}$$
$$\gamma A_i^{'}|_{x=0} + \delta B_i^{'}|_{x=0} = ik\epsilon. \tag{55}$$

Equations (50), (51), (54) and (55) are summarized in the form

$$M_1 \begin{pmatrix} \beta \\ \gamma \\ \delta \\ \epsilon \end{pmatrix} = \begin{pmatrix} 0 \\ 0 \\ 0 \\ 0 \end{pmatrix}, \tag{56}$$

where

$$M_1 = \begin{pmatrix} e^{ik^{'}a_1} & -A_i|_{x=-a_1} & -B_i|_{x=-a_1} & 0 \\ ik^{'}e^{ik^{'}a_1} & A_i^{'}|_{x=-a_1} & B_i^{'}|_{x=-a_1} & 0 \\ 0 & A_i|_{x=0} & B_i|_{x=0} & -1 \\ 0 & A_i^{'}|_{x=0} & B_i^{'}|_{x=0} & -ik \end{pmatrix}. \tag{57}$$

The resonant eigenvalues are the solutions of the the equation

$$\det M_1 = 0. \tag{58}$$

We plot in Figs. 8–10(a) $\log|\det M_1|$ as a function of $E = E_r + iE_i$ for several parameter sets. The dimples in the plots indicate the resonant eigenvalues. The numerical estimates of the eigenvalues are shown in Tables 1–3. Here we put $\hbar = 1$.

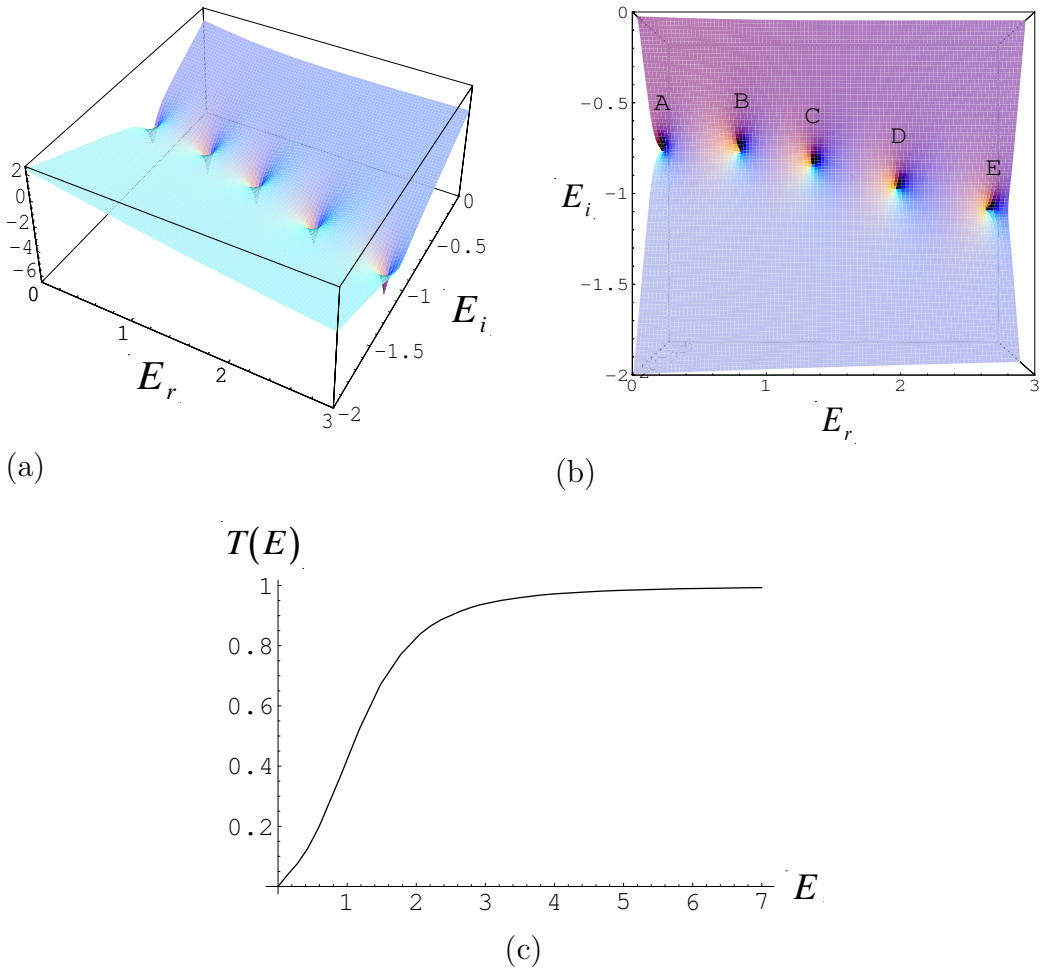

Figure 8: (a) The dimples indicate the positions of resonant states in the complex energy plane. The potential parameters are $a = 2$, $V_0 = 2$ and $V_1 = 20$. (b) The top view of (a). (c) The energy dependence of the transmission probability.

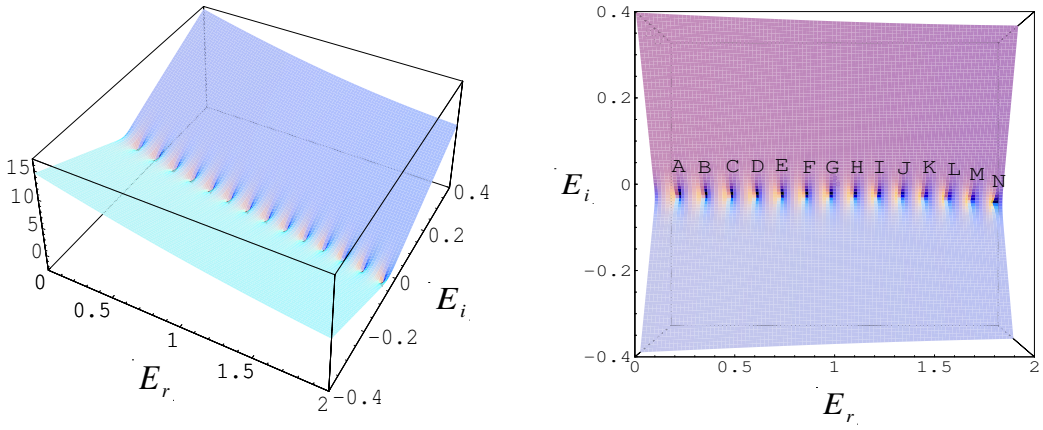

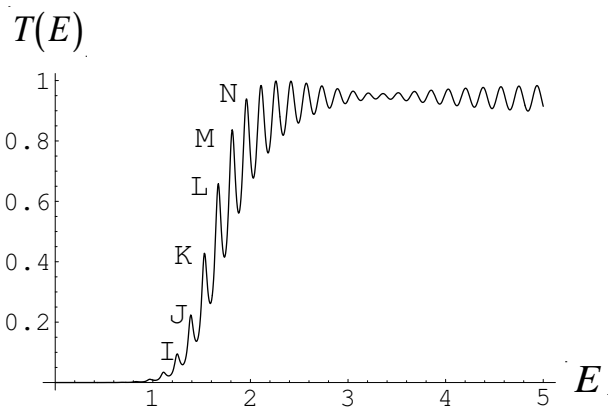

Figure 9: (a) The dimples indicate the positions of resonant states in the complex energy plane. The potential parameters are $a = 8$, $V_0 = 2$ and $V_1 = 30$. (b) The top view of (a). (c) The energy dependence of the transmission probability.

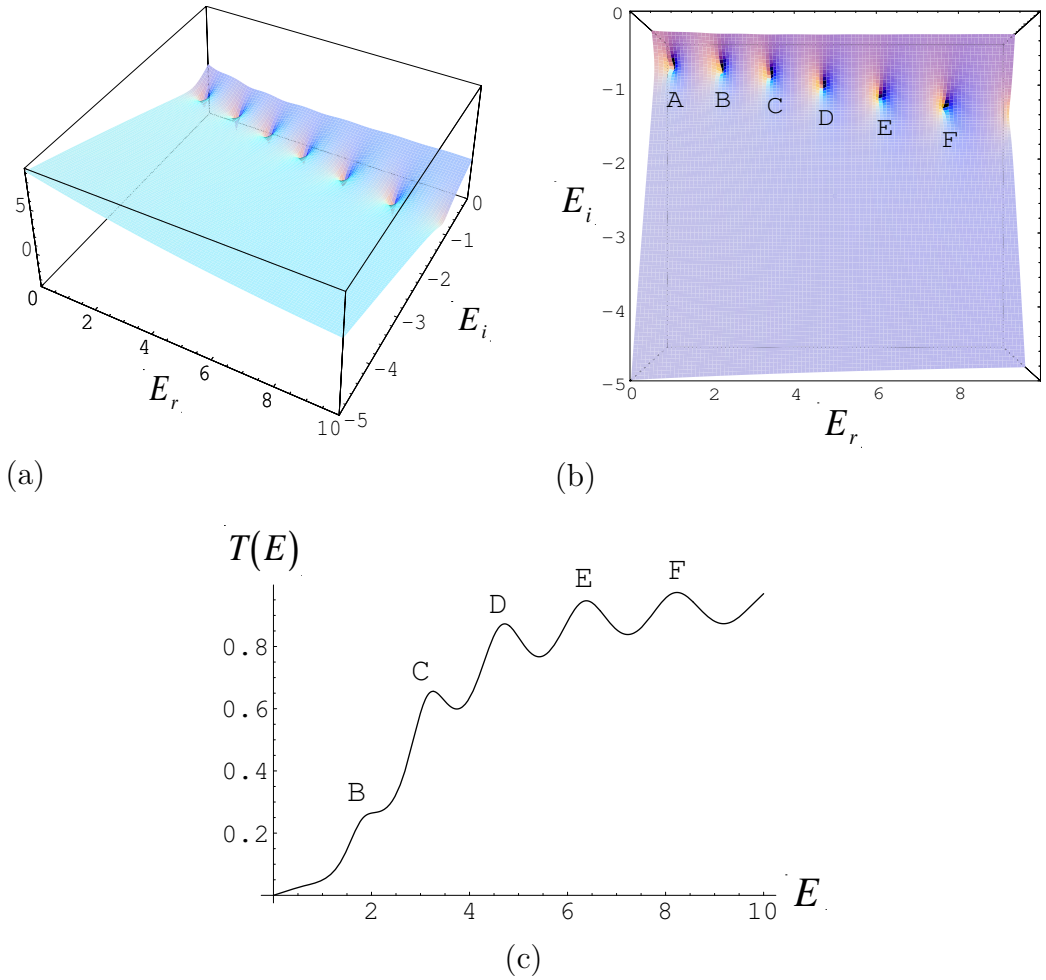

Figure 10: (a) The dimples indicate the positions of resonant states in the complex energy plane. The potential parameters are $a = 2$, $V_0 = 4$ and $V_1 = 20$. (b) The top view of (a). (c) The energy dependence of the transmission probability.

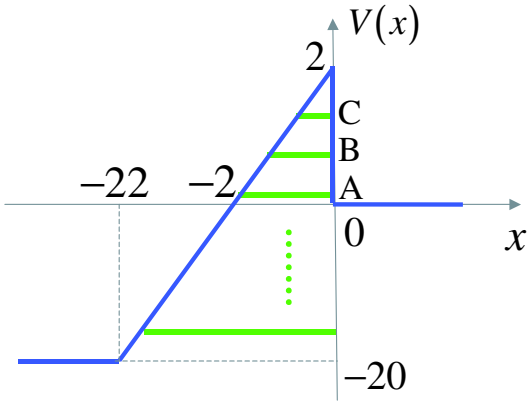

Figure 11: The resonant states inside the triangular potential. The potential parameters are $a = 2$, $V_0 = 2$ and $V_1 = 20$. The green lines A–C indicate the resonant states in the region $0 < E_r < V_0$. The eigenvalues of the resonant states A–C correspond to the ones in Table 1.

	eigenvalues	lifetime
A	$0.0123204 - 0.725906i$	0.688794
B	$0.668691 - 0.719661i$	0.694771
C	$1.31052 - 0.813337i$	0.614752
D	$2.05178 - 0.963382i$	0.519005
E	$2.87329 - 1.10478i$	0.452579

Table 1: Eigenvalues in the triangular potential in Fig. 8. The capital letters A–E correspond to the ones in Fig. 8 (b).

We find resonant states, some of which are located inside the potentials as indicated in Fig. 11; for example, in Fig. 8, three resonant states (A, B and C) in the region $0 < E_r < V_0$. (Note that we find resonant states not only as shown in Figs. 8–10 but also in the region $-V_1 < E_r < 0$.) We propose to define the tunneling time as twice the lifetimes of the resonant states A–C shown in Table 1. The lifetime of the resonant state B is the longest of all the resonant states.

We plot in Fig. 12 the position of resonant states shifting the potential parameters a and V_0, while keeping the potential slope V_0/a unchanged. We note that the resonant states inside the potential do not move as shown in Fig. 12 (b), when the potential parameters a and V_0 are changed.

We also calculate the transmission probability as follows. We first assume

resonant states			the transmission probability		
	eigenvalues	lifetime		peak position	peak height
A	$0.110814 - 0.0337756i$	14.8036	A	0.12189	1.027×10^{-6}
B	$0.253774 - 0.0336957i$	14.8387	B	0.262845	7.11×10^{-6}
C	$0.396397 - 0.0336166i$	14.8736	C	0.404652	3.8794×10^{-5}
D	$0.538684 - 0.0335389i$	14.9081	D	0.546252	0.000184972
E	$0.680638 - 0.033463i$	14.9419	E	0.686866	0.000792
F	$0.822255 - 0.0334002i$	14.97	F	0.828707	0.00307558
G	$0.963523 - 0.0333714i$	14.9829	G	0.969458	0.0108186
H	$1.10442 - 0.0334517i$	14.9469	H	1.10984	0.0341876
I	$1.24494 - 0.033827i$	14.7811	I	1.24991	0.0950405
J	$1.38517 - 0.0348767i$	14.3729	J	1.38966	0.224078
K	$1.52552 - 0.0371568i$	13.4565	K	1.52963	0.429549
L	$1.66682 - 0.0411267i$	12.1576	L	1.67068	0.658974
M	$1.81011 - 0.0467853i$	10.6871	M	1.8138	0.837398
N	$1.95614 - 0.0536976i$	9.3114	N	1.95972	0.939643

Table 2: Comparison between eigenvalues in the triangular potential and the peak positions of the transmission probability in Fig. 9. The capital letters A–N correspond to the ones in Fig. 9.

resonant states			the transmission probability		
	eigenvalues	lifetime		peak position	peak height
A	$0.367546 - 0.479006i$	1.04383	A	–	–
B	$1.72488 - 0.489104i$	1.02228	B	1.91688	0.26
C	$3.09429 - 0.58705i$	0.851716	C	3.25509	0.655869
D	$4.60643 - 0.75236i$	0.664575	D	4.71808	0.872763
E	$6.30015 - 0.919728i$	0.543639	E	6.38363	0.947941
F	$8.16525 - 1.07157i$	0.466605	F	8.23269	0.973696

Table 3: Comparison between eigenvalues in the triangular potential and the peak positions of the transmission probability in Fig. 10. The capital letters A–F correspond to the ones in Fig. 10.

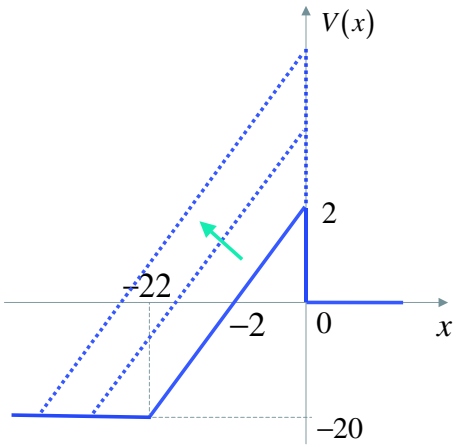

(a)

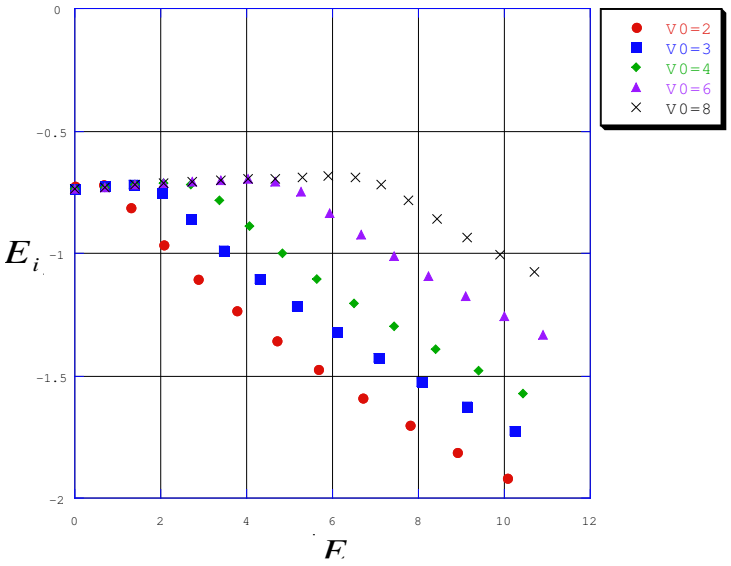

(b)

Figure 12: (a) The triangular potential with the potential parameters a and V_0 shifted and the potential slope $V_0/a = 1$ kept. (b) The position of resonant states for the potential (a). The potential height is changed as $V_0 = 2, 3, 4, 6$ and 8.

the solution of the form

$$\psi(x) = \begin{cases} \xi e^{ik^{'}x} + \rho e^{-ik^{'}x} & (x < -a_1), \\ \sigma A_i + \upsilon B_i & (-a_1 \leq x \leq 0), \\ \omega e^{ikx} & (x > 0), \end{cases} \tag{59}$$

where ξ, ρ, σ, υ and ω are coefficients. We next solve the Schrödinger equation. The transmission probability is defined as

$$T \equiv \frac{|j_t|}{|j_i|}, \tag{60}$$

where j_t and j_i are the transmission flux and the incident flux, respectively:

$$j \equiv \frac{\hbar}{m}\mathrm{Re}\psi^* p\psi = \frac{\hbar}{2mi}(\psi^*\nabla\psi - \psi\nabla\psi^*). \tag{61}$$

Thus we have

$$|j_i| = \frac{\hbar k^{'}}{m}|\xi|^2, \tag{62}$$

$$|j_t| = \frac{\hbar k}{m}|\omega|^2, \tag{63}$$

which is followed by

$$T = \frac{k}{k'}\frac{|\omega|^2}{|\xi|^2}. \tag{64}$$

We show the results in Figs. 8–10(c). Incidentally, the energy E is real in computing the transmission probability, so that the momentum flux is automatically conserved:

$$k^{'}|\xi|^2 = k^{'}|\rho|^2 + k|\omega|^2. \tag{65}$$

The transmission probability in Fig. 8 lacks any peaks, probably because the imaginary parts of the eigenvalues are comparatively large. In Figs. 9 and 10, on the other hand, the transmission probability exhibits several peaks, which is close to the real part of the resonant states as shown in Tables 2 and 3. We discuss in Appendix A the relation between the position of the resonant state and the peak.

4.2 A potential with a flat top

We here show resonant states and its lifetime in a potential shown in Fig. 13, taking more account of experimental situations. The potential for the actual

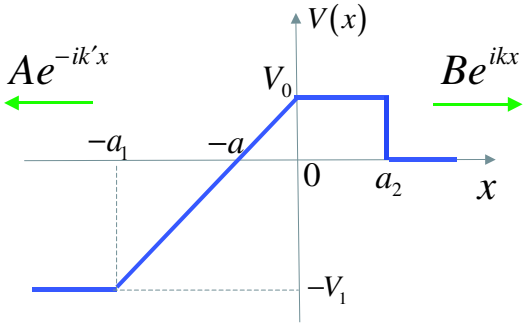

Figure 13: A flat-top potential. The potential parameters a, a_1, a_2, V_0 and V_1 are all positive.

field emission (Fig. 7) may be of a shape where the top of the triangular potential (Fig. 6) is flattened out.

Similarly to the case of the triangular potential, we consider the solution of the Schrödinger equation

$$\left\{-\frac{\hbar^2}{2m}\frac{\partial^2}{\partial x^2}+V(x)\right\}\psi(x)=E\psi(x), \tag{66}$$

where the potential is given by

$$V(x)=\begin{cases} -V_1 & (x<-a_1) \\ \frac{V_0}{a}x+V_0 & (-a_1\le x\le 0) \\ V_0 & (0<x\le a_2) \\ 0 & (x>a_2) \end{cases}, \tag{67}$$

with

$$a_1\equiv\frac{V_0+V_1}{V_0}a. \tag{68}$$

(i) In the region $x<-a_1$, Eq. (66) is reduced to

$$\left\{-\frac{\hbar^2}{2m}\frac{\partial^2}{\partial x^2}-V_1\right\}\psi_1(x)=E\psi_1(x). \tag{69}$$

The solution is

$$\psi_1(x)=\zeta e^{-ik'x}, \tag{70}$$

where ζ is a constant and

$$k'\equiv\frac{\sqrt{2m(E+V_1)}}{\hbar}. \tag{71}$$

Note that we here used the boundary condition of the outgoing waves only, in order to search resonant states. Hence in this region, we have only the left-going wave in Eq. (70).

(ii) In the region $-a_1 \leq x \leq 0$, the general solution is given by the Airy functions as

$$\psi_2(x) = \eta A_i + \theta B_i, \tag{72}$$

where η and θ are constants.

(iii) In the region $0 < x \leq a_2$, Eq. (66) is

$$\left(-\frac{\hbar^2}{2m}\frac{\partial^2}{\partial x^2} + V_0\right)\psi_3(x) = E\psi_3(x) \tag{73}$$

$$\frac{\partial^2\psi_3(x)}{\partial x^2} = \frac{2m(V_0 - E)}{\hbar^2}\psi_3(x). \tag{74}$$

The solution is

$$\psi_3(x) = \lambda e^{\kappa x} + \mu e^{-\kappa x}, \tag{75}$$

where λ and μ are constants and

$$\kappa \equiv \frac{\sqrt{2m(V_0 - E)}}{\hbar}. \tag{76}$$

(iv) In the region $x > a_2$, Eq. (66) is

$$-\frac{\hbar^2}{2m}\frac{\partial^2\psi_4(x)}{\partial x^2} = E\psi_4(x). \tag{77}$$

The solution is

$$\psi_4(x) = \nu e^{-ikx}, \tag{78}$$

where ν is a coefficient and

$$k \equiv \frac{\sqrt{2mE}}{\hbar}. \tag{79}$$

We have only the right-going wave due to the boundary condition for resonant states.

Now we fix the constants ζ, η, θ, λ, μ and ν with the boundary conditions at $x = -a_1$, $x = 0$ and $x = a_2$. The boundary conditions at $x = -a_1$ are

$$\psi_1(-a_1) = \psi_2(-a_1), \tag{80}$$

$$\psi_1'(-a_1) = \psi_2'(-a_1), \tag{81}$$

or

$$\zeta e^{ik^{'}a_1} = \eta A_i|_{x=-a_1} + \theta B_i|_{x=-a_1}, \quad (82)$$

$$-ik^{'}\zeta e^{ik^{'}a_1} = \eta A_i^{'}|_{x=-a_1} + \theta B_i^{'}|_{x=-a_1}. \quad (83)$$

Similarly, the boundary conditions at $x = 0$ are

$$\psi_2(0) = \psi_3(0), \quad (84)$$

$$\psi_2^{'}(0) = \psi_3^{'}(0), \quad (85)$$

or

$$\eta A_i|_{x=0} + \theta B_i|_{x=0} = \lambda + \mu, \quad (86)$$

$$\eta A_i^{'}|_{x=0} + \theta B_i^{'}|_{x=0} = \kappa\lambda - \kappa\mu. \quad (87)$$

The boundary conditions at $x = a_2$ are

$$\psi_3(a_2) = \psi_4(a_2), \quad (88)$$

$$\psi_3^{'}(a_2) = \psi_4^{'}(a_2), \quad (89)$$

or

$$\lambda e^{\kappa a_2} + \mu e^{-\kappa a_2} = \nu e^{ika_2}, \quad (90)$$

$$\kappa\lambda e^{\kappa a_2} - \kappa\mu e^{-\kappa a_2} = ik\nu e^{ika_2}. \quad (91)$$

Equations (82), (83), (86), (87), (90) and (91) are summarized in the form of

$$M_2 \begin{pmatrix} \zeta \\ \eta \\ \theta \\ \lambda \\ \mu \\ \nu \end{pmatrix} = \begin{pmatrix} 0 \\ 0 \\ 0 \\ 0 \\ 0 \\ 0 \end{pmatrix}, \quad (92)$$

where

$$M_2 = \begin{pmatrix} e^{ik^{'}a_1} & -A_i|_{x=-a_1} & -B_i|_{x=-a_1} & 0 & 0 & 0 \\ ik^{'}e^{ik^{'}a_1} & A_i^{'}|_{x=-a_1} & B_i^{'}|_{x=-a_1} & 0 & 0 & 0 \\ 0 & A_i|_{x=0} & B_i|_{x=0} & -1 & -1 & 0 \\ 0 & A_i^{'}|_{x=0} & B_i^{'}|_{x=0} & -\kappa & \kappa & 0 \\ 0 & 0 & 0 & e^{\kappa a_2} & e^{-\kappa a_2} & -e^{ika_2} \\ 0 & 0 & 0 & \kappa e^{\kappa a_2} & -\kappa e^{-\kappa a_2} & -ike^{ika_2} \end{pmatrix}. \quad (93)$$

The resonant eigenvalues are the solutions of the the equation

$$\det M_2 = 0. \quad (94)$$

We show eigenvalues thus obtained for the flat-top potential in Fig. 14 and Table 4. We plot in Fig. 14 (a) $\log|\det M_2|$ as a function of $E = E_r + iE_i$.

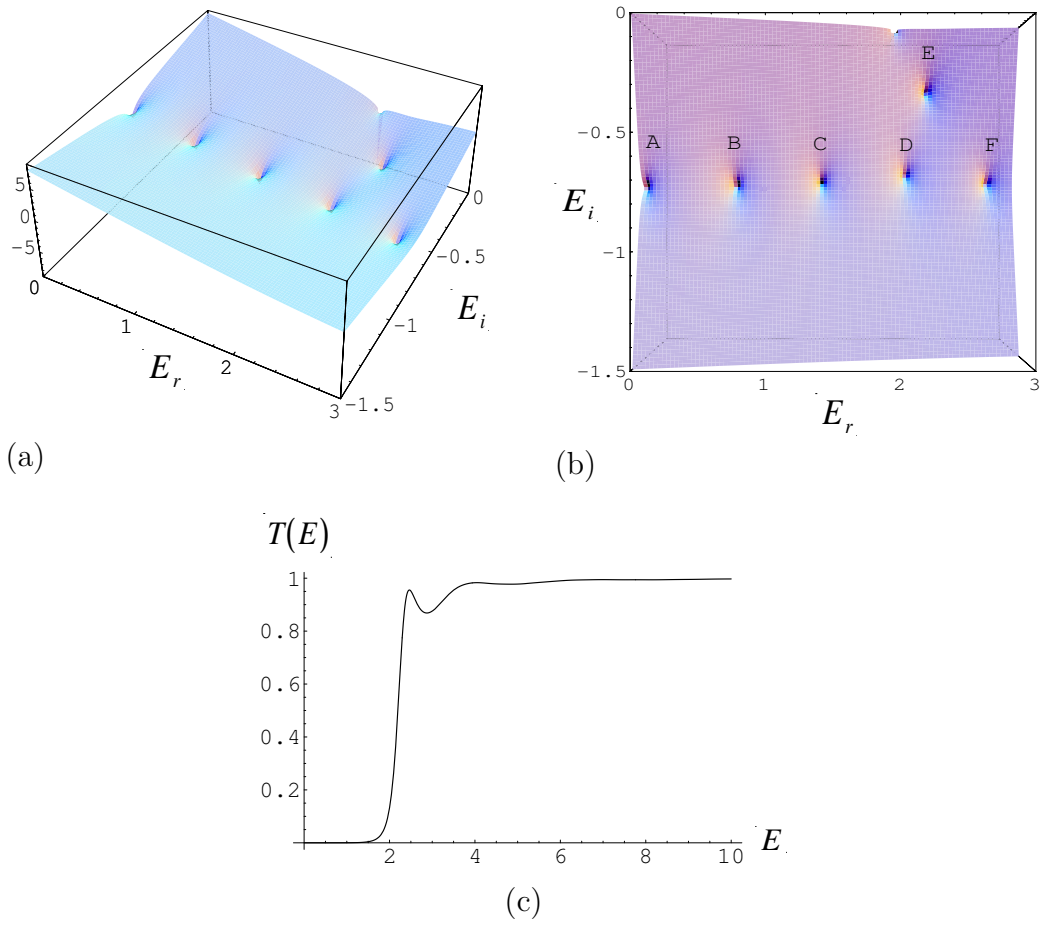

Figure 14: (a) The dimples indicate the positions of resonant states in the complex energy plane. The potential parameters are $a = 2$, $a_2 = 4$, $V_0 = 2$ and $V_1 = 20$. (b) The top view of (a). (c) The energy dependence of the transmission probability.

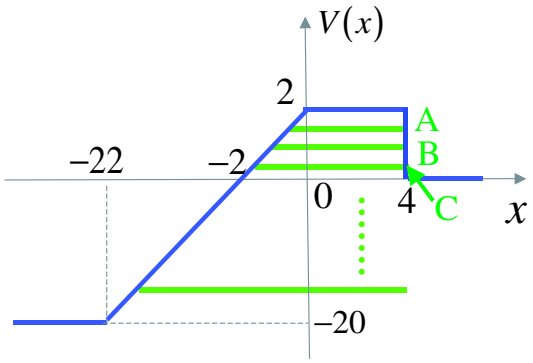

Figure 15: The resonant states inside the flat-top potential. The potential parameters are $a = 2$, $a_2 = 4$, $V_0 = 2$ and $V_1 = 20$. The green lines A–C indicate the resonant states in the region $0 < E_r < V_0$. The eigenvalues of the resonant states A–C correspond to the ones in Table 4.

	eigenvalues	τ
A	$0.0153786 - 0.734706i$	0.680544
B	$0.71218 - 0.727131i$	0.687634
C	$1.40054 - 0.714486i$	0.699804
D	$2.10592 - 0.678247i$	0.737195
E	$2.28302 - 0.279677i$	1.78778
F	$2.80367 - 0.717486i$	0.696878

Table 4: Eigenvalues in the flat-top potential. The capital letters A–F correspond to the ones in Fig. 14 (b).

We find resonant states, some of which are located inside the potential, similar to the case of the triangular potential as indicated in Fig. 15. We find in Fig. 14, three resonant states (A, B and C) in the region $0 < E_r < V_0$. We propose to define the tunneling time as twice the lifetimes of the resonant states A–C shown in Table 4.

We find in Fig. 16 (b) that some resonant states in the region $0 < E_r < V_0$ do not change when the potential width a_2 is changed as $a_2 = 2, 3, 4, 6$ and 8 as shown in Fig. 16 (a), while keeping the other parameters unchanged. In contrast, the resonant states in the region $E_r > V_0$ depend on the parameters significantly.

We also plot the resonant states (Fig. 17 (b)), shifting the potential parameters a and V_0 as shown in Fig. 17 (a), while the potential slope $V_0/a = 1$ and the width $a_2 = 2$ kept. We find that resonant states inside the poten-

tial do not move. As the real part of the eigenvalue increases, however, the eigenvalues get scattered.

We find a "floating" resonant state E in Fig. 14(b) and a peak in Fig. 14(c). The imaginary part of the resonant state E is particularly smaller than the one of the other resonant states as shown in Table 4. We consider that the resonant state E contributes to the peak in Fig. 14(c). The peak of the transmission probability is

$$\begin{cases} E = 2.46471, \\ T(E) = 0.955409. \end{cases} \tag{95}$$

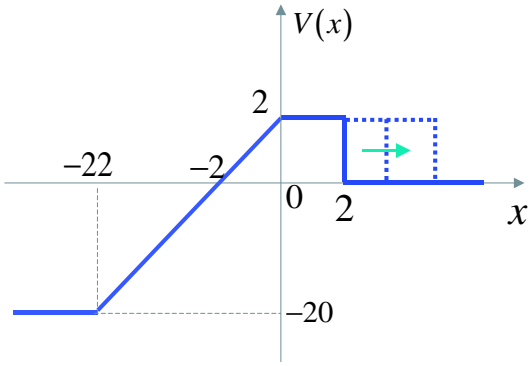

(a)

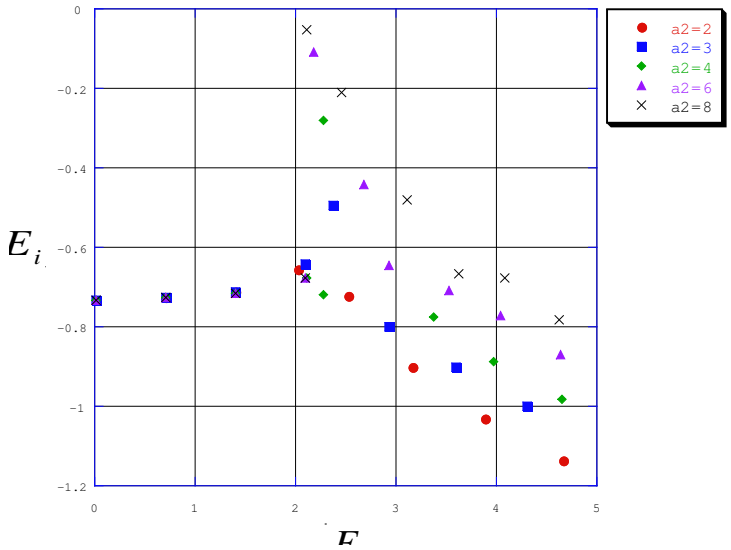

(b)

Figure 16: (a) The flat-top potential with the potential width a_2 shifted. (b) The position of resonant states for the potential (a). The potential width is changed as $a_2 = 2, 3, 4, 6$ and 8.

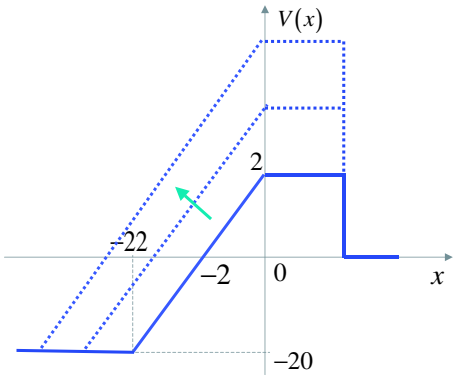

(a)

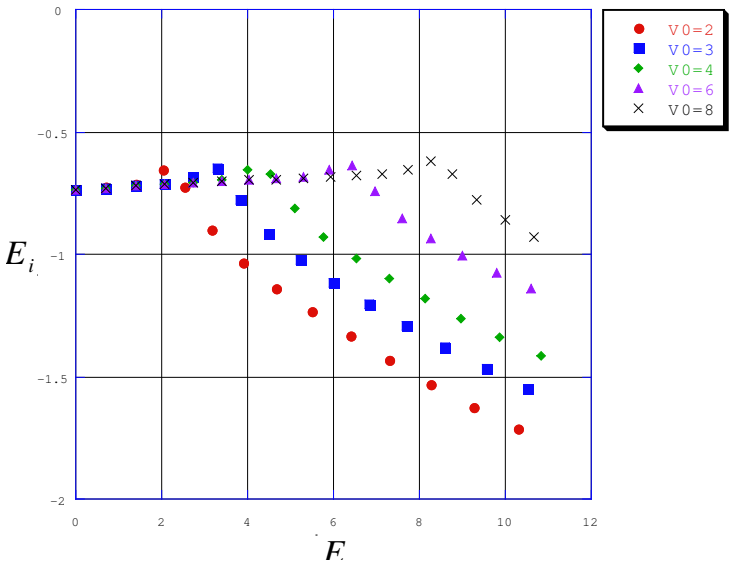

(b)

Figure 17: (a) The flat-top potential with the potential parameters a and V_0 shifted, while the potential slope $V_0/a = 1$ and the width $a_2 = 2$ kept. (b) The position of resonant states for the potential (a). The potential height is changed as $V_0 = 2, 3, 4, 6$ and 8.

4.3 A semi-infinite triangular potential

We here show resonant states and its lifetime in a potential shown in Fig. 18. In the region $x < 0$, the potential continues infinitely.

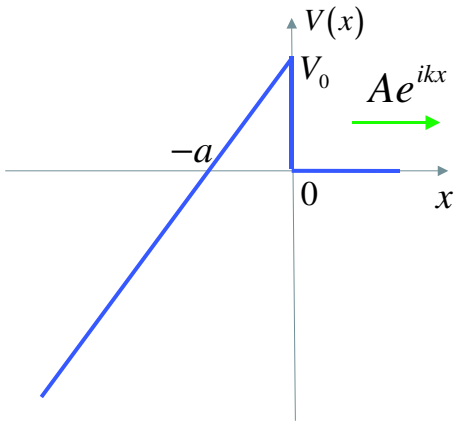

Figure 18: A semi-infinite triangular potential. The potential parameters a and V_0 are all positive.

Let us solve the Schrödinger equation

$$\left\{-\frac{\hbar^2}{2m}\frac{\partial^2}{\partial x^2} + V(x)\right\}\psi(x) = E\psi(x), \tag{96}$$

where the potential is given by

$$V(x) = \begin{cases} \frac{V_0}{a}x + V_0 & (x \leq 0) \\ 0 & (x > 0) \end{cases}. \tag{97}$$

(i) In the region $x \leq 0$, we transform the way to solve the Schrödinger equation in the same way as in (ii) of Section 4.1. The general solution $\psi_1(x)$ in this region is a superposition of the two Airy functions:

$$\psi_1(x) = B_i + iA_i, \tag{98}$$

Note that we here used the boundary condition of the outgoing waves only, in order to search resonant states. The asymptotic forms of the Airy functions in $x \to -\infty$ are given by

$$A_i(z) \approx \frac{1}{\sqrt{\pi}}(-z)^{-\frac{1}{4}}\sin\left\{\frac{2}{3}(-z)^{\frac{3}{2}} + \frac{\pi}{4}\right\}, \tag{99}$$

$$B_i(z) \approx \frac{1}{\sqrt{\pi}}(-z)^{-\frac{1}{4}}\cos\left\{\frac{2}{3}(-z)^{\frac{3}{2}} + \frac{\pi}{4}\right\}, \tag{100}$$

where

$$z \equiv \alpha^{\frac{1}{3}}(x+X), \tag{101}$$

$$X \equiv a - \frac{a}{V_0}E. \tag{102}$$

Hence Eq. (98) is asymptotically given by

$$\psi_1(x) \approx \frac{1}{\sqrt{\pi}}(-z)^{-\frac{1}{4}} e^{i\left\{\frac{2}{3}(-z)^{3/2}+\frac{\pi}{4}\right\}}, \tag{103}$$

which is a left-going wave only.

(ii) In the region $x > 0$, Eq. (96) is

$$-\frac{\hbar^2}{2m}\frac{\partial^2\psi_2(x)}{\partial x^2} = E\psi_2(x). \tag{104}$$

The solution is

$$\psi_2(x) = \beta e^{-ikx}, \tag{105}$$

where β is a constant and

$$k \equiv \frac{\sqrt{2mE}}{\hbar}. \tag{106}$$

We have only the right-going wave because of the boundary condition for resonant states.

Now we fix the constants β with the boundary conditions at $x = 0$. The boundary conditions at $x = 0$ are

$$\psi_1(0) = \psi_2(0), \tag{107}$$

$$\psi_1^{'}(0) = \psi_2^{'}(0), \tag{108}$$

or

$$A_i|_{x=0} + B_i|_{x=0} = \beta, \tag{109}$$

$$A_i^{'}|_{x=0} + B_i^{'}|_{x=0} = ik\beta. \tag{110}$$

By substituting Eq. (109) for β in Eq. (110), we have

$$M_3 = B_i^{'}|_{x=0} + kA_i|_{x=0} + i\left(A_i^{'}|_{x=0} - kB_i|_{x=0}\right) = 0. \tag{111}$$

We shows eigenvalues thus obtained for the semi-infinite triangular potential in Fig. 19 and Table 5. We plot in Fig. 19 (a) $\log M_3$ as a function of $E = E_r + iE_i$. Here we put $\hbar = 1$.

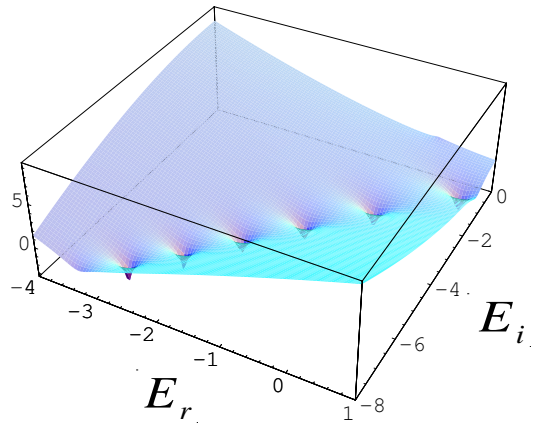

(a)

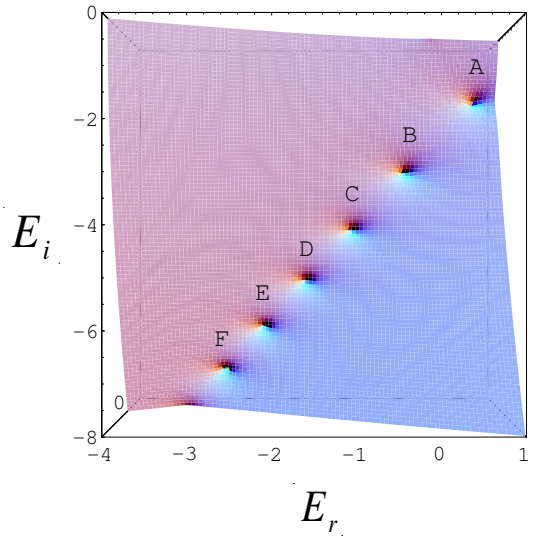

(b)

Figure 19: (a) The dimples indicate the position of resonant states in the complex energy plane. The potential parameters are $a = 2$ and $V_0 = 2$. (b) The top view of (a).

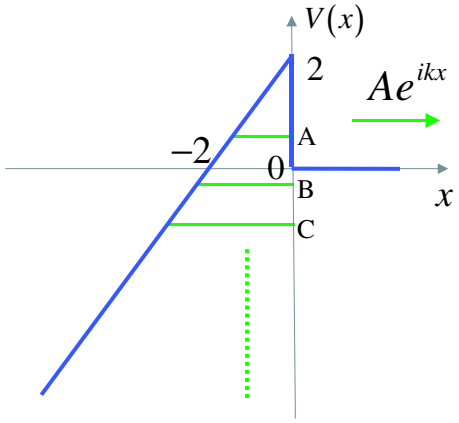

Figure 20: The resonant states inside the semi-infinite triangular potential. The potential parameters are $a = 2$ and $V_0 = 2$. The eigenvalues of the resonant states A–C (green lines) correspond to the ones in Table 5.

	eigenvalues	τ
A	$0.735064 - 1.26171i$	0.396288
B	$-0.241223 - 2.8479i$	0.175568
C	$-0.988344 - 4.14562i$	0.120609
D	$-1.63417 - 5.282i$	0.0946611
E	$-2.21901 - 6.31419i$	0.0791867
F	$-2.76136 - 7.27174i$	0.0687593

Table 5: Eigenvalues in the semi-infinite potential. The capital letters A–F correspond to the ones in Fig. 19 (b).

We find resonant states, some of which are located inside the potential as indicated in Fig. 20. We find only one resonant state (the state A) in the region $0 < E_r < V_0$ and do not find states in the region $E_r > V_0$. On the other hand, an infinite number of the resonant states exist in the region $E_r < 0$. The lifetime of the resonant state A is the longest of all the resonant states as shown in Table 5.

5 Summary

We obtain the resonant states for several potentials, some of which are located inside the potential. We propose to define the tunneling time as twice the lifetime of the resonant states. The resonant state with the longest lifetime in the triangular potential exists in the region $0 < E_r < V_0$. Our results for the triangular potential may be comparable to field-emission measurements.

We also changed the potential parameters. We stress that the resonant states inside the potential do not move when we keep the potential slope constant. For the flat-top potential, the resonant states inside the potential do not depend on the potential width. Finally, the transmission probability exhibits several peaks, which is close to the real part of the resonant states.

Acknowledgments

I would like to thank Associate Professor N.Hatano for kind guidance and many pieces of advice. Owing to your help, I could be absorbed in the research.

A The relation between the position of a resonant state and the Lorentz peak

We here discuss the relation between the position of a resonant state and a peak of the transmission probability.

Suppose that we have a complex eigenvalue

$$\lambda = \alpha - i\beta. \tag{112}$$

The transmission probability, on the other hand, is given by

$$T(E) \propto \left| \frac{1}{E - \mathcal{H}} \right|^2, \tag{113}$$

which has a contribution from the eigenvalue λ as

$$\begin{aligned} T(E) &\propto \frac{1}{|E - (\alpha - i\beta)|^2}, \\ &= \frac{1}{|(E - \alpha) + i\beta|^2}, \\ &= \frac{1}{(E - \alpha)^2 + \beta^2}. \end{aligned} \tag{114}$$

This leads to

$$T(\alpha) = \frac{1}{\beta^2}. \tag{115}$$

Eq. (115) represents the transmission probability in the real part of the complex eigenvalue (Fig. 21).

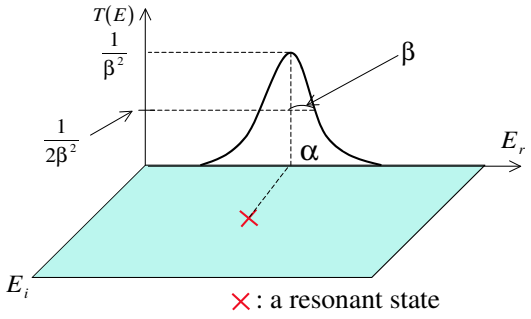

Figure 21: The position of a resonant state and a peak of the transmission probability.

Let us consider the real part of the complex eigenvalue when the transmission probability is a half of Eq. (115):

$$\frac{1}{2\beta^2} = \frac{1}{(E-\alpha)^2+\beta^2}, \tag{116}$$

$$(E-\alpha)^2 = \beta^2, \tag{117}$$

$$E = \alpha \pm \beta. \tag{118}$$

Eq. (118) represents that the imaginary part of a complex eigenvalue (Eq. 112) corresponds to the half width. Thus the width of the transmission probability is greater for the greater imaginary part of a complex eigenvalue.

References

[1] R. Landauer and T. Martin, *Barrier interaction time in tunneling*, Rev. Mod. Phys. **66**, 217–228 (1994)

[2] e.g. T. E. Hartman, J. Appl. Phys. **33**, 3247 (1962)

[3] D. Sokolovski and L.M. Baskin, *Traversal time in quantum scattering*, Phys. Rev. A **36**, 4604 (1987)

[4] M. Büttiker and R. Landauer, *Traversal time for tunneling*, Phys. Rev. Lett. **49**, 1739 (1982)

[5] N. Hatano, *Complex eigenvalues and resonant states*, unpublished.

[6] L.D. Landau and E.M. Lifshitz, *Quantum Mechanics* (3rd Edition, Pergamon Press), §134